The stability and aggregation of ovine prion protein associated with classical and atypical scrapie correlates with the ease of unwinding of helix-2

Tim J Fitzmaurice, David F Burke, Lee Hopkins, Sujeong Yang, Shuiliang Yu, Man-Sun Sy, Alana M Thackray, Raymond Bujdoso

Biochemical Journal Immediate Publication. Published on 12 Oct 2007 as manuscript BJ20071122

The stability and aggregation of ovine prion protein associated with classical and atypical scrapie correlates with the ease of unwinding of helix-2

Tim J. Fitzmaurice*, David F. Burke†, Lee Hopkins*, Sujeong Yang*, Shuiliang Yu‡, Man-Sun Sy‡, Alana M. Thackray* and Raymond Bujdoso*[1]

*** Department of Veterinary Medicine**
University of Cambridge, Madingley Road, Cambridge, CB3 OES, UK

† Department of Biochemistry, University of Cambridge
Tennis Court Road, Cambridge, CB2 1GA, UK

‡ Department of Pathology, School of Medicine, Case Western Reserve University
10900 Euclid Avenue, Cleveland, OH 44106, USA

[1] Corresponding author

(Tel: 44-1223-337655; Fax 44-1223-337610; email: rb202@cam.ac.uk)

Running title: Helix-2 influences prion protein stability

PrPC / polymorphism / transmissible spongiform encephalopathies / protease / conformational stability

ABBREVIATIONS

AF141RQ, A136 F141 R154 Q171; AHQ, A136 H154 Q171; AL141RQ, A136 L141 R154 Q171; ARR, A136 R154 R171; VRQ, V136 R154 Q171; BCA, bicinchoninic acid; BSE, Bovine spongiform encephalopathy; CDI, conformation dependent immunoassay; CJD, Creutzfeldt-Jakob Disease; cps, counts per second; GdnHCl, guanidine hydrochloride; GSS, Gerstmann-Sträussler-Scheinker disease; *mds*, molecular dynamics simulations; PK, proteinase K; PrP, prion-related protein; PrPC, normal cellular form of PrP; PrPSc, abnormal disease-specific conformation of PrP; *rmsf*, root-mean-squared fluctuations.

SUMMARY

Susceptibility to scrapie disease in sheep, the archetypal prion disease, correlates with polymorphisms within the ovine PrP gene. The VRQ and AL141RQ allelic variants are associated with classical scrapie, whilst the ARR, AF141RQ and AHQ allelic variants are associated with atypical scrapie. Recent studies have suggested that there are differences in the stability of PrPSc associated with these different forms of scrapie. To address which structural features of ovine PrP may contribute to this difference, we have investigated the conformational stability and susceptibility to aggregation of allelic variants of ovine PrP associated with classical or atypical scrapie. We find that the melting temperature of ovine recombinant VRQ and AL141RQ PrP is higher than that of AF141RQ, AHQ and ARR. In addition, monoclonal antibody studies show that the region around helix-1 of VRQ and AL141RQ is less accessible compared to other ovine PrP allelic variants. Furthermore, the extent of both the structural change to copper ion-treatment and denaturant-induced aggregation was reduced in PrP associated with atypical scrapie compared to PrP associated with classical scrapie. Through the use of molecular dynamics simulations we have found that these biochemical and biophysical properties of ovine PrP correlate with the ease of unwinding of helix-2 and a concurrent conformational change of the helix-2 - helix-3 loop. These data reveal significant differences in the overall stability and potential for aggregation of different allelic variants of ovine PrP and consequently have implications for the differences in stability of PrPSc associated with classical and atypical scrapie.

INTRODUCTION

Prion diseases, such as scrapie in sheep, bovine spongiform encephalopathy (BSE) in cattle and Creutzfeldt-Jakob Disease (CJD) in humans, are transmissible chronic neurodegenerative disorders. Collectively, these diseases may be inherited, arise sporadically or occur through environmental exposure to infectious prion material [1]. All of these prion diseases are considered to share the same pathogenic mechanism, which involves the misfolding and aggregation of the normal host protein PrPC into a polymeric β-sheet rich form termed PrPSc. Although the primary structure of PrPC and PrPSc appear identical, they have significantly different biophysical properties. PrPC is soluble in detergent and readily digested by proteases whereas PrPSc can be insoluble in detergent and relatively resistant to proteolytic digestion [2]. PrPC is predominantly α-helical with little β-sheet, whilst PrPSc has considerably more β-sheet content and a similar α-helical content [3]. The protein-only hypothesis postulates that PrPSc is the transmissible prion agent [4].

The disease-associated form of PrP accumulates in prion-affected individuals principally in the form of amorphous aggregates. Furthermore, it has recently been shown that smaller aggregates are more infectious than larger oligomeric forms of PrPSc giving weight to the view that the deposition of mature fibrillar amyloid aggregates of PrPSc is a protective mechanism to avoid the high intrinsic toxicity of soluble oligomers [5]. The mechanism of misfolding and aggregation of PrP remains to be established. Structural studies of PrP have been conducted in order to understand the underlying molecular mechanism and to identify possible structural intermediates of the conversion process of PrPC to PrPSc. NMR structures of recombinant PrP from a variety of mammalian species [6] and of native bovine PrPC [7] have been described, as have the crystal structures of the globular domain of human [8] and ovine recombinant PrP [9]. Collectively, these structural analyses show that PrP consists of a flexible N-terminal region followed by a globular C-terminal domain, both approximately 100 amino acids in length. The C-terminal domain of the normal form of PrP comprises three α-helices, inter-dispersed by a short anti-parallel β-sheet region. In contrast, the detailed secondary structure analysis of PrPSc has been hampered because of its insolubility. Instead, the structure of PrPSc has been inferred from comparative protein folding studies with other amyloidogenic proteins. In general, misfolded amyloidogenic proteins tend to adopt a fibrillar form that displays a common cross-β structure with β-strands perpendicular and β-sheet parallel to the fibril axis [10]. Using this framework, several models of PrPSc have been proposed [11-13]. In all cases, the modelled PrPSc has a

significant increase in β-sheet compared to the native structure of PrPC suggesting that the normal form of PrP undergoes an α-helical to β-strand conversion before, or during, fibril formation.

Scrapie of sheep is the archetypal prion disease and dimorphisms in ovine PrP at amino acid residues 136, 154 and 171 are associated with differences in susceptibility to classical scrapie [14, 15]. Animals that express the allelic variant V136R154Q171 (in short, VRQ, where V, R, and Q stand for valine, arginine, and glutamine) or A136L141R154Q171 (AL141RQ, where A and L stand for alanine and leucine, respectively) show susceptibility to classical scrapie while those with A136R154R171 (ARR) show resistance. The biochemical and physicochemical properties of these allelic variants of ovine recombinant PrP have been analyzed [16, 17]. These studies revealed that PrP protein of the scrapie-susceptible genotypes VRQ and AL141RQ has a more compact structure and higher thermal denaturation temperature compared to resistant ARR protein. Despite this difference in thermodynamic stability, all three ovine PrP genotypes can form amyloidogenic intermediates in an acidic as well as neutral environment [18]. However, the rate of formation and β-sheet content of the amyloidogenic intermediates are affected by the ovine PrP polymorphisms, and both show a positive correlation with scrapie susceptibility. Recently, asymptomatic and symptomatic atypical scrapie, that is clearly distinguishable from classical scrapie infection, have been identified in sheep with A136F141R154Q171 (AF141RQ, where F stands for phenylalanine) and A136H154Q171 (AHQ, where H stands for histidine) PrP alleles [19, 20]. Significantly, the PrPSc that accumulates in cases of atypical scrapie is less Proteinase K (PK)-resistant than its counterpart in classical scrapie [21].

The molecular mechanism that accounts for the variation in susceptibility to classical or atypical scrapie, and the difference in proteolytic susceptibility exhibited by PrPSc in these different forms of scrapie remain unknown. However, critical amino acid residues will clearly influence the extent or stability of structural changes within normal forms of ovine PrP, its proteolytic stability or its functional interaction with potential co-factors, as it converts to any given disease-associated form of PrP. While the precise details are not yet fully established, various regions in the PrP molecule have been implicated as important to structural change and helix-1 appears to be significantly linked to aggregation [22-24]. It therefore follows that it may be possible to identify genotype-specific differences in structure and potentially correlate them to disease associated biophysical activity, such as aggregation. We, and others, have previously shown that allelic variants of ovine PrP associated with susceptibility and

resistance to classical scrapie have different biophysical properties and different responses to copper, a perceived ligand of the prion protein [16-18]. Ovine VRQ PrP showed a significant increase in β-sheet content when exposed to copper whereas ARR protein remained relatively unchanged [17]. Here we have extended these studies and have compared the stability and aggregation of the different genotypic forms of ovine PrP associated with either classical or atypical scrapie. Importantly, we have found that those allelic variants associated with atypical scrapie show an increase in accessibility to epitopes in the C-terminal of the molecule, and a lower potential to aggregate compared with those allelic variants associated with classical scrapie. In addition we have carried out molecular dynamics simulations (*mds)* that reveal this dichotomy correlates with the ease of unwinding of helix-2.

MATERIALS AND METHODS

Generation of ovine recombinant PrP

Full-length ovine recombinant PrP (AF141RQ, AL141RQ, AHQ, ARR, or VRQ) (amino acid residues 25 - 232), was generated as described previously [17] in a method adapted from Hornemann et al [25]. Oxidized and refolded recombinant PrP was stored at -80 ˚C.

Anti-PrP monoclonal antibodies

The generation, purification and characterization of the anti-PrP monoclonal antibodies 8B4; 11G5; 7H6; 2C2; 8H4; 12A3; 7A12 [26-28]; SAF32 [29] and 249 [30] has been described in detail previously. Based on the human PrP sequence numbering, monoclonal antibody 8B4 recognizes an epitope between amino acid residues 37 and 44; SAF32 reacts with amino acid residues 59 - 89, covering the octapeptide repeat sequences; 11G5 reacts with amino acid residues 115 - 130 spanning β-sheet 1; 12A3 recognizes amino acid residues 120 - 136; 7H6 recognizes amino acid residues 130 - 140; 7A12 interacts with helix-1 between amino acid residue 143 and 155; 2C2 reacts with amino acid residues 153 - 165 in β-sheet 2; 8H4 recognizes amino acid residues 175 - 185 of helix-2. Monoclonal antibody 249 reacts in the N-terminal region of helix-2. All monoclonal antibodies were affinity purified using Protein G chromatography. Where required biotinylation of monoclonal antibodies was performed using the EZ-linked sulfo-*N*-hydroxysuccinimido-biotin kit (Pierce, Rockford, USA catalogue no. 21217) according to the manufacturer's recommendation.

Protein quantification

Total protein concentration of ovine recombinant PrP or anti-PrP monoclonal antibody samples was measured using the bicinchoninic-acid (BCA) assay (Pierce, Perbio Science, UK, Ltd, catalogue no. 23225) as described [31].

CD spectra

Samples of recombinant PrP at concentrations of 25 μM prepared in 50 mM sodium acetate were used for CD spectroscopic analysis. All samples were centrifuged at 13000 *g* at 4 ˚C for 30 min prior to analysis. CD spectra were recorded in a 0.5 mm length quartz cuvette at either 20 ˚C, or the specified temperature, under constant nitrogen flushing using a Jasco 810 spectropolarimeter. At least 10 spectra were accumulated and the values were expressed as molar ellipticity (θ). Quantitative β-sheet content was determined from deconvoluted CD spectroscopic data using the CONTINLL programme [32].

Direct ELISA

Direct ELISA was carried out as described previously [31].

Capture - detector immunoassay

Capture - detector immunoassay was carried out as described by Yin et al. [28] with the following modifications. Purified capture monoclonal antibody 12A3 was coated at 50 ng/well in 96-well flat-bottomed plates for 16 h at 4 ˚C. Excess antibody was removed and wells were blocked with PBS containing 3 % BSA for 2 h at 20 ˚C. Plates were washed three times with PBS containing 0.05 % Tween 20 (PBS-T20) and 200 ng/well of ovine recombinant PrP in PBS (pH 7.4) were captured for 1 h at 20 ˚C. The remainder of the protocol was as described by Yin et al. [28]. Each experiment was repeated at least three times.

Western blot analysis of ovine recombinant PrP

Western blot analysis of recombinant PrP was carried out as described previously [24]. PrP bands were detected by enhanced chemiluminescence.

Metal ion-treatment of ovine recombinant PrP

Stocks of recombinant PrP in sodium acetate buffer were diluted to 20 μM in water and incubated with either 200 μM or 2 mM copper or manganese sulphate at 37 ˚C for 20 h. Metal ion-treated samples were incubated at 4 ˚C for a further 5 days prior to use.

Turbidity measurement

The aggregation reactions were performed according to Frankenfield et al. [33] with minor modifications. The assays were performed at 37 ˚C in a volume of 200 μl/well in 96-well plates. AL141RQ and AHQ allelic variants of ovine recombinant PrP were suspended in 50 mM sodium acetate supplemented with 150 mM NaCl (pH 4.0). The solutions were pre-incubated at 37 ˚C before mixing. Guanidine hydrochloride (GdnHCl) was added to a final concentration of 0.5 M to initiate the aggregation reaction. After addition of GdnHCl, turbidities were monitored within 15 sec by reading the absorbance at 405 nm in a Beckman Coulter AD340 micro-ELISA plate reader, using a kinetic photometric model (interval time 50 sec, 60 cycles with 1 sec shaking before every cycle).

Comparative modelling molecular dynamics simulations (*mds*)

Models of the C-terminal domain (residues 119 - 228) of the AHQ, AF141RQ, AL141RQ, ARR and VRQ allelic variants of ovine PrP were built using the program MODELLER [34]

using default parameters based upon the X-ray structure of ovine PrP [9]. The *mds* were carried out with the program Gromacs [35] using the OPLS-AA/L all-atom force field as previously described [36].

Nomenclature

Amino acid residue numbers refer to the ovine PrP sequence unless otherwise stated.

RESULTS

Expression and purification of ovine recombinant PrP

We have generated allelic variants of ovine PrP associated with classical or atypical scrapie in order to compare the biophysical and biochemical properties of these different proteins. Full-length ovine VRQ, AL141RQ, ARR, AF141RQ and AHQ recombinant PrP (amino acid residues 25 - 232) were cloned by PCR, expressed in the bacterial expression vector pET-23b, and purified by metal chelate and ion-exchange chromatography using a method adapted from Hornemann et al. [25]. Oxidatively refolded genotypic forms of ovine recombinant PrP were of the correct apparent molecular weight, namely 23kDa and were predominantly in the monomeric state as determined by size exclusion chromatography (SEC), which verified the solubility of ovine PrP at the pH conditions used in this study [16] (and data not shown). Far-UV CD spectral analysis was used to determine secondary protein structure of the refolded recombinant PrP molecules. CD spectra of full-length ovine recombinant PrP displayed maxima UV absorbance peaks at 208 and 222 nm, typical of the predominantly α-helical structure expected for ovine PrP (data not shown) [16, 25]. Although the CD spectra of these different genotypic forms of ovine PrP showed similar α-helical structure, a difference was seen in the thermal stability of these proteins. CD spectra of full-length PrP proteins heated from 20 ˚C to 95 ˚C showed that conversion of the α-helical structure to random coil varied in a genotypic manner. Table 1 shows that the transition temperature (t_m) of VRQ occurred at 74 ˚C and for AL141RQ at a t_m of 71 ˚C. In contrast, ovine recombinant PrP variants associated with atypical scrapie had an average t_m of 69 ˚C. These data show that whilst the overall structure of the allelic variants of ovine PrP was similar, VRQ and AL141RQ PrP appeared thermodynamically more stable and probably more compact compared to that of AF141RQ, AHQ and ARR. The stability of VRQ PrP was a feature of the core structure of the molecule as the truncated form of this protein displayed a similar t_m value as that of the full-length protein [17].

Conformational differences between allelic variants of ovine PrP

The difference in melting temperatures between ovine PrP associated with classical or atypical scrapie may reflect differences in the conformation of these various PrP proteins. In order to assess this we probed the conformation of ovine recombinant PrP with a panel of anti-PrP monoclonal antibodies to investigate whether genotypic structural differences could be detected by variation in epitope exposure. Figure 1a shows the predicted epitope location of the N- and C-terminal-specific anti-PrP monoclonal antibodies used in the present study.

We first investigated the reactivity of the panel of anti-PrP monoclonal antibodies with the various allelic variants of ovine PrP by western blot analysis. Figure 1b shows that all of the anti-PrP monoclonal antibodies generally reacted equally well with the different genotypes of ovine PrP. Monoclonal antibody 7A12 reacted less well with the AHQ protein and 8H4 less well with the VRQ allelic variant. Since the epitope for 7A12 is located within helix-1 it is possible that H154 influences the reactivity of this monoclonal antibody. The lower reactivity of monoclonal antibody 8H4 with the VRQ allelic variant suggests this protein adopts a unique conformation that is retained during SDS/PAGE and western blotting as there are no genotypic differences between the PrP allelic variants in the region of the 8H4 epitope.

The various allelic variants of ovine PrP were subsequently analyzed by capture-detector ELISA, which utilized the C-terminal specific anti-PrP monoclonal antibody 12A3 for capture and either an N-terminal specific or C-terminal-specific anti-PrP monoclonal antibody for detection. Figure 2 shows that all of the different genotypes of ovine recombinant PrP were recognized with similar efficiency when detected by the N-terminal-specific monoclonal antibody SAF32 (Figure 2a). Differences in reactivity were seen when C-terminal-specific monoclonal antibodies were used for detection (Figure 2b-d). For example ARR and AF141RQ showed more reactivity with monoclonal antibodies 7A12 (Figure 2b), 2C2 (Figure 2c) or 7H6 (Figure 2d) as detector than do VRQ and AL141RQ. This suggests that the accessibility of the epitopes in and around helix-1 of the PrP molecule are somewhat differentially exposed within allelic variants of ovine PrP. The generally lower reactivity of C-terminal-specific monoclonal antibody detectors with the AHQ molecule may reflect a unique conformation of specific epitopes within this allelic variant of PrP.

Immunoreactivity of metal ion-treated ovine recombinant PrP

We have previously described the effect of various metal ions on the overall conformation of certain allelic variants of ovine PrP [17]. Copper-treatment was found to induce more extensive β-sheet conformation in the VRQ allelic variant of ovine PrP compared to ARR protein. Furthermore, this metal-ion induced increase in β-sheet structure of ovine recombinant PrP correlated with a decreased reactivity with C-terminal-specific anti-PrP monoclonal antibodies raised to copper-refolded PrP. These data indicated genotypic differences in the response to copper-treatment by ovine recombinant PrP that correlated with susceptibility or resistance to classical scrapie. In order to determine whether allelic variants of ovine PrP associated with either classical or atypical scrapie showed a difference in response to copper-treatment we analyzed their metal ion-induced conformational change

by ELISA with anti-PrP monoclonal antibodies following treatment with copper. Figure 3a shows that copper-treated AL141RQ was recognized less efficiently by the C-terminal specific monoclonal antibody 249 than control treated protein. This effect was dependent upon the concentration of copper ion used to treat AL141RQ recombinant PrP as the effect was diminished when the concentration of metal ion used was reduced. Figure 3b shows that treatment of AL141RQ with manganese resulted in a more limited reduction in immunoreactivity with monoclonal antibody 249 at both concentrations of metal ion used, in particular when relatively high levels of PrP were assessed. This suggested that copper induced a more pronounced conformational change in ovine PrP than did manganese. Figures 3c and 3d show that treatment of AHQ recombinant PrP with either copper or manganese resulted in a more limited reduction of immunoreactivity compared to that seen with AL141RQ. Treatment of AF141RQ recombinant PrP with either copper or manganese resulted in a reduction of immunoreactivity that was intermediate to that seen with AL141RQ and AHQ (data not shown). These metal ion-induced conformational changes in ovine recombinant PrP were seen with various N- and C-terminal-specific anti-PrP monoclonal antibodies (data not shown).

Since we have previously shown [17] copper-treatment of ovine PrP does not lead to metal ion-induced precipitation [37], we speculated that the observed decreased immunoreactivity was a consequence of aggregation of ovine recombinant PrP with a concomitant decrease in epitope exposure. In order to test this we investigated the ability of AL141RQ and AHQ ovine PrP to undergo denaturation-induced aggregation. These two allelic variants differ by a R154H substitution in helix-1, a critical region implicated in the oligomerization of the prion protein during conversion of PrPC to PrPSc [24, 38, 39]. Accordingly, we tested the rate and extent of aggregation of AL141RQ and AHQ proteins following their denaturation with GdnHCl. Figure 4 shows that, on addition of GdnHCl, both AL141RQ and AHQ recombinant PrP protein were capable of aggregation. However, AL141RQ showed a higher rate of aggregation than AHQ protein, although with time both proteins showed the same extent of aggregation in this assay system.

Collectively, these data indicate that PrP associated with classical and atypical scrapie show differences in their interaction with metal ions and their potential to undergo aggregation.

The stability of ovine PrP is influenced by the unwinding of helix-2

In order to investigate the structural features of ovine PrP that may account for the variation in stability and aggregation of ovine PrP we have analyzed amino acid residues 119 - 228 of all of the ovine allelic variants tested here by molecular dynamics simulations (*mds*). Figure 5 shows the average root-mean-squared fluctuations (*rmsf*) of the main-chain atoms (N,Cα,C,O) for each amino acid over the simulation. The region with the most structural variation comprises amino acid residues 190 - 205, which encompasses the C-terminal region of helix-2 and the loop between helix-2 and helix-3. The AF141RQ and AHQ alleles show the least variation in this region, whereas the AL141RQ and VRQ allelic variants show the most variation. The structural variation in the C-terminal region of helix-2 is likely to be a consequence of its "frustrated" helical conformation and its propensity to exist in an extended β-strand configuration [22, 40-42].

In the *mds* starting structures for all of the allelic variants analyzed here, helix-2 contained 6 turns. The helical conformation of the last two turns of helix-2 (H^{190}TVTTTTK^{197}) were stabilized by additional intra-helical polar interactions between the side-chain atoms of amino acid residues Thr191, Thr194, Thr195 and Thr196. The C-terminal amino acid residue of helix-2, Lys197, formed a capping interaction with the side-chain and carboxyl oxygen atoms of Thr193. Further stabilization was provided by a cluster of charged interactions involving His190 in helix-2, Glu199 of the helix-2 - helix-3 loop and amino acid residues Ala119 and Ala121. Figure 6a shows that amino acid residues Tyr158 and Arg159 of the loop preceding β-strand-2 also interacted with the backbone oxygen of Gly198 in the helix-2 - helix-3 loop. Notably, throughout the observed simulations, the last two turns of helix-2 were seen to unwind to varying degrees in a genotypic-specific manner. During the *mds* of AL141RQ (Figure 6b) and VRQ (data not shown), the angle between the N-terminal region of helix-2 and the last two turns of this helix gradually increased. Eventually, this resulted in a conformational change of amino acid residues His190 - Lys197 causing them to adopt an extended conformation (coloured in magenta in Figure 6b). The loss of the helical capping interaction between Lys197 and Thr193 allowed the concurrent unwinding of the C-terminal region of helix-2. VRQ unwound the most with the resultant shortest length of helix-2 at 3.5 turns, whilst AL141RQ unwound less to leave a slightly longer helix-2 of 4 turns. The C-terminal region of the ARR helix-2 unwound the least to leave a helix-2 of 4.5 turns. In contrast, in the allelic variants AF141RQ and AHQ, which are associated with atypical scrapie, there did not appear to be any change in the length of helix-2 as both maintained 6 helical turns.

The major determinant of the structural dichotomy shown by helix-2 was the conformational change of the helix-2 - helix-3 loop. The flexibility displayed by the helix-2 - helix-3 loop was determined principally by the orientation and packing of Lys197, Glu199, His190 and Phe201. Loss of this flexibility was precipitated by the loss of the helical capping interaction between Lys197 and Thr193, which results in a resistance to the unfolding of helix-2. For example, as shown in Figure 7, the presence of a Phe in AF141RQ (Figure 7a) allows the formation of an extended aromatic-stacking interaction between Phe141, His143, Tyr153 of helix-1, and Tyr160 of β-strand-2. Consequently, helix-1 is rotated by 30° compared to its position in AL141RQ (Figure 7b), thereby providing a further energy barrier to the unfolding or structural re-arrangement of β-strand-1, helix-1 and β-strand-2. Loss of this flexibility was precipitated by the loss of the helical capping interaction between Lys197 and Thr193. In both the AL141RQ and VRQ alleles, the new conformation of the helix-2 - helix-3 loop was stabilized by interactions between the side-chains of Thr193, Thr195, Thr196 and Lys197 of helix-2 with the backbone nitrogen or oxygen atoms of amino acid residues Ala119, Ala122, Ala124, Val125 and Gln189.

The result of this conformational change in the C-terminal region of helix-2 was the formation of a β-hairpin structure by the helix-2 - helix-3 loop and its subsequent interaction with an extended conformation of amino acid residues 119 - 130 that results in the formation of a 3 stranded β-sheet structure (data not shown). Although not quantifiable, the extended β-sheet rich-structure was only readily apparent in some of the *mds* of the VRQ and ARQ allelic variants during the time scale of the analysis carried out here.

Biochemical Journal Immediate Publication. Published on 12 Oct 2007 as manuscript BJ20071122

DISCUSSION

Scrapie, like other forms of transmissible prion disease, is characterized by the conversion of the normal cellular protein PrPC into the abnormal isomer PrPSc. Various allelic variants of ovine PrP are associated with classical or atypical scrapie. Furthermore, PrPSc from classical scrapie is more resistant to proteolytic digestion than is its counterpart that accumulates in atypical scrapie. The relatively PK-sensitive PrPSc associated with the atypical cases of scrapie does transmit to ovine PrP transgenic mice, indicating that this material is indeed transmissible [21]. However, the molecular explanation for the difference in proteolytic stability between different allelic variants of ovine PrP associated with these various forms of scrapie remains to be established.

In order to begin to address this issue, we have generated genotypic variants of ovine recombinant PrP protein via a prokaryotic expression system to investigate their conformational stability and susceptibility to aggregation. These recombinant proteins were correctly refolded into predominantly α-helical conformation as shown by CD spectral analysis, in accordance with other species forms of PrP [3, 16]. Despite overall structural similarity, the different allelic variants of ovine PrP protein showed genotypic differences in thermal stability as judged by unfolding of the α-helical structure. Our previous data and results by others have shown that ovine VRQ PrP is more compact and thermodynamically more stable than ARR protein [9, 16-18, 36]. Here we have shown by thermal denaturation that the allelic variants VRQ and ARQ were characterized by a higher t_m than AF141RQ, AHQ and ARR. These data indicate that ovine PrP associated with susceptibility to classical scrapie was thermodynamically more stable than that associated with susceptibility to atypical scrapie. Paradoxically, the enhanced thermal stability of ovine PrP associated with susceptibility to classical scrapie was also accompanied by a greater potential for conformational variation as shown by a greater capacity to form β-sheet structure. We have previously shown that following treatment with copper the VRQ allelic variant is predisposed to more β-sheet formation compared to ARR [17]. Furthermore, differences in the unfolding of these classical scrapie-susceptible and -resistant forms of PrP are known to exist. VRQ unfolding intermediates exhibit β-sheet structure whilst those of the ARR variant display random coil structure [18]. Here we have shown that the AL141RQ allelic variant undergoes greater conformational change following treatment with copper than do the allelic variants AF141RQ and AHQ. This would suggest that those allelic variants of ovine PrP associated with susceptibility to classical scrapie, rather than atypical scrapie, are more susceptible to

accumulate in a disease-associated form. This is supported by our observation that AL141RQ recombinant PrP aggregates more readily than does AHQ protein.

Collectively, these observations support the view that differences in the metabolism of allelic variants of ovine PrP contribute to the mechanism(s) that determine susceptibility and resistance of sheep to scrapie [9, 18]. Furthermore, the genotypic difference in PrP stability would also appear to correlate with susceptibility to classical and atypical scrapie. The emergence of atypical scrapie in sheep with PrP genotypes that are associated with resistance to classical scrapie, including ARR, indicates that these allelic variants of ovine PrP are capable of conversion to a disease-associated form. However, the deposition of PrPSc in atypical cases of scrapie is different from that seen in classical cases of scrapie. Significantly, atypical cases of scrapie are usually characterized by the absence of PrPSc at peripheral sites including lymphoid tissue. This would imply that whilst the majority, if not all, of the genotypes of ovine PrP are capable of conversion to PrPSc, the mechanism(s) of metabolic resistance to some forms of scrapie operates at a peripheral site. In such a scheme, the thermodynamically less stable allelic variants would be efficiently metabolized before they were able to accumulate in any significant amount in a disease-associated form. In support of this, it has been shown in brain homogenates that VRQ PrPC is more resistant to PK digestion than ARR protein [43]. Furthermore, our own preliminary experiments have suggested that AL141RQ ovine recombinant PrP is more resistant to PK digestion compared to the allelic variants AF141RQ and AHQ (data not shown). These observations tentatively suggest that the proteolytic sensitivity of PrPSc associated with classical or atypical scrapie may, in part, be a reflection of an inherent difference in stability of the different genotypic forms of ovine PrP associated with these various forms of scrapie. It is also possible that this genotypic difference in structural stability contributes to the apparent selective interaction of different scrapie prion strains with different ovine PrP allelic variants.

It is clear that polymorphic amino acid substitutions in ovine PrP influence the structural stability of the prion protein. We have used *mds* in order to predict the range of structural conformations adopted by different allelic variants of ovine PrP that may account for the observed differences in their stability. In our studies reported here, we have found that the ease of unfolding of the C-terminus of helix-2 is allele-specific and is associated with a concurrent conformational change of the helix-2 - helix-3 loop. Furthermore, we predict that a consequence of the unfolding of helix-2 is the formation of a β-hairpin structure by the helix-2 - helix-3 loop and its subsequent interaction with an extended conformation of amino acid

residues 119 - 130 that results in the formation of a 3 stranded β-sheet structure. The extended β-sheet structure comprises amino acid residues 119 - 130; β-sheet-1; β-sheet-2; the C-terminal region of helix-2 and the helix-2 - helix-3 loop. One consequence of the formation of this extended β-sheet structure is the restriction of movement of amino acid residues 119 - 130. This will in turn limit accessibility to the major protease cleavage site, which is located in this region of the protein [44]. Conversely, any hindrance to the unfolding of helix-2 in ovine PrP would be expected to lead to an increase in proteolytic susceptibility of the prion protein. Mechanisms of resistance to the unfolding of helix-2 were evident in those allelic variants associated with atypical scrapie. The presence of a buried Phe at amino acid residue 141 in AF141RQ forces a re-orientation of the peptide segment comprising amino acid residues Val136 –> Try153, which includes helix-1. The presence of His154 in the AHQ allele causes a change of side-chain conformation of neighbouring helix-1 residues His143, Phe144 and Arg151. These similar conformational changes seen in both AF141RQ and AHQ subsequently displaced the extended peptide segment comprising residues 119 - 130. As a consequence, this results in the absence of interactions, notably with residues on helix-1 and Asn162 on β-strand-2 and the amino acid residues 119 - 125, which were seen to stabilize the conformation of the helix-2 - helix-3 loop following the unwinding of helix-2 in the AL141RQ and VRQ allelic variants. The ARR allelic variant of ovine PrP shows a limited propensity to unwind in the C-terminal region of helix-2 but does not readily form an extended β-sheet-rich structure. We have shown that the repulsion between Arg171 and Arg167 in the ARR allele forces a re-orientation of Tyr131 that subsequently forms an interaction with Gln189 in helix-3. The presence of Tyr131 packed between β-strand-2 and helix-3 is likely to block the movement of peptide 119 - 130, which as seen in the AL141RQ and VRQ allele, is required to interact with the β-hairpin conformation of the helix-2 - helix-3 loop and nucleate the formation of the extended β-sheet rich structure.

A common feature of those allelic variants that show a low propensity to unwind in the C-terminal region of helix-2 are proposed conformational differences in the region of helix-1 compared to VRQ and AL141RQ. These proposed conformational differences correlate with differences in epitope exposure between the different allelic variants, in particular in the central portion of ovine recombinant PrP as revealed by data from the capture-detector immunoassay. Helix-1, which is extremely hydrophilic and has a high propensity to adopt a helical structure, has been implicated in the aggregation process of PrP [24, 38, 39] although its role is unclear. It has been suggested that helix-1 unwinds during the conversion of PrPC into PrPSc to provide more β-sheet structure [39, 45] or may be involved in intermolecular

salt bridges during aggregation of PrPSc [38]. Our *mds* observations suggest that certain allelic variants of the normal form of the ovine prion protein PrPC have the capacity to adopt a significant level of β-sheet structure, above that exhibited by β-strand-1 and β-strand-2, in the absence of modification by a prion disease-specific agent or co-factor. The existence of C-terminal folding intermediates of human recombinant PrP that could represent pre-aggregation states of the protein have been described [46]. In addition, Lu et al. [47] describe the presence of a β-sheet core in the C-terminal region of human recombinant PrP that has been folded into amyloid fibrils. Our mds reported here predict that formation of the extended β-sheet structure in ovine PrP does not require the immediate unfolding of helix-1. This suggests that the extended β-sheet structure predicted here for ovine PrP represents a normal conformation of the prion protein that would be expected to be present in prion-free brain tissue. This view is consistent with the observation that detergent-insoluble PrPC aggregates that contain PK-resistant core fragments are detectable in normal human brain tissue [48]. We speculate that the β-strands that result as a consequence of structural re-arrangement of the C-terminal region of helix-2 and the helix-2 - helix-3 loop of ovine PrP contribute to the structural stability of aggregated PrPSc molecules. In such a scheme, the PrPSc that arises from the VRQ or AL141RQ allelic forms of ovine PrP, which show the greatest propensity to unwind in the C-terminal region of helix-2, would be stabilized to a greater extent than PrPSc comprising other allelic variants of ovine PrP that do not show such a propensity to unfold in this region. An extension of this proposal is that the structural restraints offered by each allelic variant toward formation of the extended β-strand-rich PrP intermediate in normal ovine PrP, contributes to the regulation of their conversion to PrPSc by different ovine scrapie strains. On this basis, the allele-specific conformational stability of ovine PrP and the ability to interact with different ovine scrapie prion strains appear to contribute to the regulation of susceptibility and resistance to scrapie disease in sheep.

ACKNOWLEDGEMENTS

This work was supported in part by grants from the Defra and the Wellcome Trust.
LH is in receipt of a Defra PhD studentship. The PhD studentship of SY is in part supported by funds from the Cambridge Overseas Trust.

LEGENDS

Table 1. Transitional temperature (t_m) at 222 nm of ovine recombinant PrP

Transitional temperatures of PrP variants were obtained from analysis of a temperature denaturation curve read at 222 nm for each allelic variant, using the Sigmaplot software package. The transitional value (t_m) was the temperature halfway between the minima and maxima of the denaturation curve. Results are shown as mean (t_m) in ˚C ± SD.

Figure 1a. Epitope location of anti-PrP monoclonal antibodies

The location of anti-PrP monoclonal antibody-binding epitopes along the length of PrP. LS, leader sequence; GPI, glycosyl phosphatidylinositol anchor; β, β-strand.

Figure 1b. Western blot of ovine recombinant PrP

Ovine recombinant PrP was separated by SDS/PAGE under reducing conditions and subsequently immunoblotted with monoclonal antibodies 8B4, 12A3, 11G5, 8H4 and 7A12.

Figure 2. Capture-detector ELISA of ovine recombinant PrP

Ovine recombinant PrP VRQ (△); AL141RQ (◇); AF141RQ (○); ARR (□); AHQ (✳) were captured on ELISA plates which had been coated with monoclonal antibody 12A3 at 50 ng/well. After washing with PBS-T20, various concentrations of biotinylated monoclonal antibody (a) SAF32; (b) 7A12; (c) 2C2 and (d) 7H6 were added to the plates followed by HRP-conjugated streptavidin. Absorbance at 405 nm was determined. The data presented represent the means of triplicate wells ± SD and are a representative data set from three replicate experiments.

Figure 3. Immunoreactivity of metal ion-treated ovine recombinant PrP

Ovine recombinant AL141RQ PrP (a) and (b); or AHQ PrP (c) and (d); was treated with water (■) or either 200 μM (●) or 2 mM (▲) copper (a) and (c) or manganese (b) and (d) at 37 ˚C as described in the Materials and Methods. Subsequently, serial 2-fold dilutions of recombinant PrP were analyzed for reactivity with the anti-PrP monoclonal antibody 249 by direct ELISA. The data presented represent the means of triplicate wells ± SD.

Figure 4. PrP aggregation assay

GdnHCl (0.5 M) was added to 4 μM of AL141RQ (●) or AHQ (○) ovine recombinant PrP in 50 mM sodium acetate and 150 mM NaCl (pH 4.0). The aggregation kinetics were

monitored by the increase in absorbance at 405 nm at 37 ˚C.

Figure 5. Root-mean-squared fluctuations (*rmsf*) of the main-chain atoms for amino acid residues in the C-terminal region of different ovine PrP allelic variants

Coloured lines represent: AHQ (red); AL141RQ (blue); AF141RQ (green); ARR (violet); VRQ (black).

Figure 6. Side-chain interactions in the C-terminal region of helix-2 of AL141RQ

(a) Snapshot at 1.5 ns. A cluster of charged interactions involving His190, Glu199, Tyr158 and Arg159 help stabilize the end of helix-2 and the conformation of the helix-2 - helix-3 loop. (b) At 15 ns, the last two turns of helix-2 unwind with a conformational change of the helix-2 - helix-3 loop. With a concurrent movement of the peptide comprising amino acid residues 119 - 130 (coloured in cyan), an extended β-sheet is formed with the new conformation of the helix-2 - helix-3 loop.

Figure 7. Steric hindrance prevents unwinding of helix-2 in AF141RQ

The dimorphism present in (a) AF141RQ causes an extended aromatic-stacking interaction between Phe141, His143, Tyr153 of helix-1, and Tyr160 of β-strand-2. As a consequence, helix-1 is rotated 30° compared to its position in (b) AL141RQ. These interactions would provide an additional energy barrier to the unfolding or structural re-arrangement of β-strand-1, helix-1 and β-strand-2.

REFERENCES

1 Collinge, J. (2001) Prion diseases of humans and animals: their causes and molecular basis. Annu. Rev. Neurosci. **24**, 519-550

2 Prusiner, S. B., Groth, D. F., Bolton, D. C., Kent, S. B. and Hood, L. E. (1984) Purification and structural studies of a major scrapie prion protein. Cell **38**, 127-134

3 Pan, K. M., Baldwin, M., Nguyen, J., Gasset, M., Serban, A., Groth, D., Mehlhorn, I., Huang, Z., Fletterick, R. J., Cohen, F. E. and et al. (1993) Conversion of alpha-helices into beta-sheets features in the formation of the scrapie prion proteins. Proc. Natl. Acad. Sci. USA **90**, 10962-10966

4 Prusiner, S. B. (1982) Novel proteinaceous infectious particles cause scrapie. Science **216**, 136-144

5 Silveira, J. R., Raymond, G. J., Hughson, A. G., Race, R. E., Sim, V. L., Hayes, S. F. and Caughey, B. (2005) The most infectious prion protein particles. Nature **437**, 257-261

6 Lysek, D. A., Schorn, C., Nivon, L. G., Esteve-Moya, V., Christen, B., Calzolai, L., von Schroetter, C., Fiorito, F., Herrmann, T., Guntert, P. and Wuthrich, K. (2005) Prion protein NMR structures of cats, dogs, pigs, and sheep. Proc. Natl. Acad. Sci. USA **102**, 640-645

7 Hornemann, S., Schorn, C. and Wuthrich, K. (2004) NMR structure of the bovine prion protein isolated from healthy calf brains. EMBO Rep. **5**, 1159-1164

8 Knaus, K. J., Morillas, M., Swietnicki, W., Malone, M., Surewicz, W. K. and Yee, V. C. (2001) Crystal structure of the human prion protein reveals a mechanism for oligomerization. Nat. Struct. Biol. **8**, 770-774

9 Eghiaian, F., Grosclaude, J., Lesceu, S., Debey, P., Doublet, B., Treguer, E., Rezaei, H. and Knossow, M. (2004) Insight into the PrPC-->PrPSc conversion from the structures of antibody-bound ovine prion scrapie-susceptibility variants. Proc. Natl. Acad. Sci. USA **101**, 10254-10259

10 Sunde, M., Serpell, L. C., Bartlam, M., Fraser, P. E., Pepys, M. B. and Blake, C. C. (1997) Common core structure of amyloid fibrils by synchrotron X-ray diffraction. J. Mol. Biol. **273**, 729-739

11 DeMarco, M. L. and Daggett, V. (2004) From conversion to aggregation: protofibril formation of the prion protein. Proc. Natl. Acad. Sci. USA **101**, 2293-2298

12 Govaerts, C., Wille, H., Prusiner, S. B. and Cohen, F. E. (2004) Evidence for assembly of prions with left-handed beta-helices into trimers. Proc. Natl. Acad. Sci.

USA **101**, 8342-8347

13 Langedijk, J. P., Fuentes, G., Boshuizen, R. and Bonvin, A. M. (2006) Two-rung model of a left-handed beta-helix for prions explains species barrier and strain variation in transmissible spongiform encephalopathies. J. Mol. Biol. **360**, 907-920

14 Clouscard, C., Beaudry, P., Elsen, J. M., Milan, D., Dussaucy, M., Bounneau, C., Schelcher, F., Chatelain, J., Launay, J. M. and Laplanche, J. L. (1995) Different allelic effects of the codons 136 and 171 of the prion protein gene in sheep with natural scrapie. J. Gen. Virol. **76**, 2097-2101

15 Goldmann, W., Hunter, N., Smith, G., Foster, J. and Hope, J. (1994) PrP genotype and agent effects in scrapie: change in allelic interaction with different isolates of agent in sheep, a natural host of scrapie. J. Gen. Virol. **75**, 989-995

16 Rezaei, H., Marc, D., Choiset, Y., Takahashi, M., Hui Bon Hoa, G., Haertle, T., Grosclaude, J. and Debey, P. (2000) High yield purification and physico-chemical properties of full-length recombinant allelic variants of sheep prion protein linked to scrapie susceptibility. Eur. J. Biochem. **267**, 2833-2839

17 Wong, E., Thackray, A. M. and Bujdoso, R. (2004) Copper induces increased beta-sheet content in the scrapie-susceptible ovine prion protein PrPVRQ compared with the resistant allelic variant PrPARR. Biochem. J. **380**, 273-282

18 Rezaei, H., Choiset, Y., Eghiaian, F., Treguer, E., Mentre, P., Debey, P., Grosclaude, J. and Haertle, T. (2002) Amyloidogenic unfolding intermediates differentiate sheep prion protein variants. J. Mol. Biol. **322**, 799-814

19 Buschmann, A., Biacabe, A. G., Ziegler, U., Bencsik, A., Madec, J. Y., Erhardt, G., Luhken, G., Baron, T. and Groschup, M. H. (2004) Atypical scrapie cases in Germany and France are identified by discrepant reaction patterns in BSE rapid tests. J. Virol. Methods **117**, 27-36

20 Saunders, G. C., Cawthraw, S., Mountjoy, S. J., Hope, J. and Windl, O. (2006) PrP genotypes of atypical scrapie cases in Great Britain. J. Gen. Virol. **87**, 3141-3149

21 Le Dur, A., Beringue, V., Andreoletti, O., Reine, F., Lai, T. L., Baron, T., Bratberg, B., Vilotte, J. L., Sarradin, P., Benestad, S. L. and Laude, H. (2005) A newly identified type of scrapie agent can naturally infect sheep with resistant PrP genotypes. Proc. Natl. Acad. Sci. USA **102**, 16031-16036

22 Dima, R. I. and Thirumalai, D. (2002) Exploring the propensities of helices in PrP(C) to form beta sheet using NMR structures and sequence alignments. Biophys. J. **83**, 1268-1280

23 Watzlawik, J., Skora, L., Frense, D., Griesinger, C., Zweckstetter, M., Schulz-

Schaeffer, W. J. and Kramer, M. L. (2006) Prion protein helix1 promotes aggregation but is not converted into beta-sheet. J. Biol. Chem. **281**, 30242-30250

24 Yu, S., Yin, S., Li, C., Wong, P., Chang, B., Xiao, F., Kang, S. C., Yan, H., Xiao, G., Tien, P. and Sy, M. S. (2007) Aggregation of prion protein with insertion mutations is proportional to the number of inserts. Biochem. J. **403**, 343-351

25 Hornemann, S., Korth, C., Oesch, B., Riek, R., Wider, G., Wuthrich, K. and Glockshuber, R. (1997) Recombinant full-length murine prion protein, mPrP(23-231): purification and spectroscopic characterization. FEBS Lett. **413**, 277-281

26 Li, R., Liu, T., Wong, B. S., Pan, T., Morillas, M., Swietnicki, W., O'Rourke, K., Gambetti, P., Surewicz, W. K. and Sy, M. S. (2000) Identification of an epitope in the C terminus of normal prion protein whose expression is modulated by binding events in the N terminus. J. Mol. Biol. **301**, 567-573

27 Zanusso, G., Liu, D., Ferrari, S., Hegyi, I., Yin, X., Aguzzi, A., Hornemann, S., Liemann, S., Glockshuber, R., Manson, J. C., Brown, P., Petersen, R. B., Gambetti, P. and Sy, M. S. (1998) Prion protein expression in different species: analysis with a panel of new mAbs. Proc. Natl. Acad. Sci. USA **95**, 8812-8816

28 Yin, S., Pham, N., Yu, S., Li, C., Wong, P., Chang, B., Kang, S. C., Biasini, E., Tien, P., Harris, D. A. and Sy, M. S. (2007) Human prion proteins with pathogenic mutations share common conformational changes resulting in enhanced binding to glycosaminoglycans. Proc. Natl. Acad. Sci. USA **104**, 7546-7551

29 Feraudet, C., Morel, N., Simon, S., Volland, H., Frobert, Y., Creminon, C., Vilette, D., Lehmann, S. and Grassi, J. (2005) Screening of 145 anti-PrP monoclonal antibodies for their capacity to inhibit PrPSc replication in infected cells. J. Biol. Chem. **280**, 11247-11258

30 Thackray, A. M., Madec, J. Y., Wong, E., Morgan-Warren, R., Brown, D. R., Baron, T. and Bujdoso, R. (2003) Detection of bovine spongiform encephalopathy, ovine scrapie prion-related protein (PrPSc) and normal PrPc by monoclonal antibodies raised to copper-refolded prion protein. Biochem. J. **370**, 81-90

31 Thackray, A. M., Fitzmaurice, T. J., Hopkins, L. and Bujdoso, R. (2006) Ovine plasma prion protein levels show genotypic variation detected by C-terminal epitopes not exposed in cell-surface PrPC. Biochem. J. **400**, 349-358

32 Provencher, S. W. and Glockner, J. (1981) Estimation of globular protein secondary structure from circular dichroism. Biochemistry **20**, 33-37

33 Frankenfield, K. N., Powers, E. T. and Kelly, J. W. (2005) Influence of the N-terminal domain on the aggregation properties of the prion protein. Protein Sci. **14**, 2154-2166

34 Sali, A. and Blundell, T. L. (1993) Comparative protein modelling by satisfaction of spatial restraints. J. Mol. Biol. **234**, 779-815

35 Lindahl, E., Hess, B. and van der Spoel, D. (2001) GROMACS 3.0: A package fofr molecular simulation and trajectory analysis. J. Mol. Model. **7**, 306-317

36 Bujdoso, R., Burke, D. F. and Thackray, A. M. (2005) Structural differences between allelic variants of the ovine prion protein revealed by molecular dynamics simulations. Proteins **61**, 840-849

37 Quaglio, E., Chiesa, R. and Harris, D. A. (2001) Copper converts the cellular prion protein into a protease-resistant species that is distinct from the scrapie isoform. J. Biol. Chem. **276**, 11432-11438

38 Morrissey, M. P. and Shakhnovich, E. I. (1999) Evidence for the role of PrP(C) helix 1 in the hydrophilic seeding of prion aggregates. Proc. Natl. Acad. Sci. USA **96**, 11293-11298

39 Speare, J. O., Rush, T. S., 3rd, Bloom, M. E. and Caughey, B. (2003) The role of helix 1 aspartates and salt bridges in the stability and conversion of prion protein. J. Biol. Chem. **278**, 12522-12529

40 Dima, R. I. and Thirumalai, D. (2004) Probing the instabilities in the dynamics of helical fragments from mouse PrPC. Proc. Natl. Acad. Sci. USA **101**, 15335-15340

41 Kallberg, Y., Gustafsson, M., Persson, B., Thyberg, J. and Johansson, J. (2001) Prediction of amyloid fibril-forming proteins. J. Biol. Chem. **276**, 12945-12950

42 Langella, E., Improta, R., Crescenzi, O. and Barone, V. (2006) Assessing the acid-base and conformational properties of histidine residues in human prion protein (125-228) by means of pK(a) calculations and molecular dynamics simulations. Proteins **64**, 167-177

43 Buschmann, A., Kuczius, T., Bodemer, W. and Groschup, M. H. (1998) Cellular prion proteins of mammalian species display an intrinsic partial proteinase K resistance. Biochem. Biophys. Res. Commun. **253**, 693-702

44 Chen, S. G., Teplow, D. B., Parchi, P., Teller, J. K., Gambetti, P. and Autilio-Gambetti, L. (1995) Truncated forms of the human prion protein in normal brain and in prion diseases. J. Biol. Chem. **270**, 19173-19180

45 Safar, J., Roller, P. P., Gajdusek, D. C. and Gibbs, C. J., Jr. (1993) Conformational transitions, dissociation, and unfolding of scrapie amyloid (prion) protein. J. Biol. Chem. **268**, 20276-20284

46 Kachel, N., Kremer, W., Zahn, R. and Kalbitzer, H. R. (2006) Observation of intermediate states of the human prion protein by high pressure NMR spectroscopy.

BMC Struct. Biol. **6**, 16

47 Lu, X., Wintrode, P. L. and Surewicz, W. K. (2007) Beta-sheet core of human prion protein amyloid fibrils as determined by hydrogen/deuterium exchange. Proc. Natl. Acad. Sci. USA **104**, 1510-1515

48 Yuan, J., Xiao, X., McGeehan, J., Dong, Z., Cali, I., Fujioka, H., Kong, Q., Kneale, G., Gambetti, P. and Zou, W. Q. (2006) Insoluble aggregates and protease-resistant conformers of prion protein in uninfected human brains. J. Biol. Chem. **281**, 34848-34858

Biochemical Journal Immediate Publication. Published on 12 Oct 2007 as manuscript BJ20071122

Table 1. Transitional temperature (t_m) at 222 nm of ovine recombinant PrP

PrP Genotype	Mean t_m (°C) ± SD
ARR	69.8±2.5
AHQ	68.8±1.5
AF141RQ	69.5±0.0
AL141RQ	70.8±1.3
VRQ	74.0±0.0

Biochemical Journal Immediate Publication. Published on 12 Oct 2007 as manuscript BJ20071122

Figure 1a. Epitope location of anti-PrP monoclonal antibodies

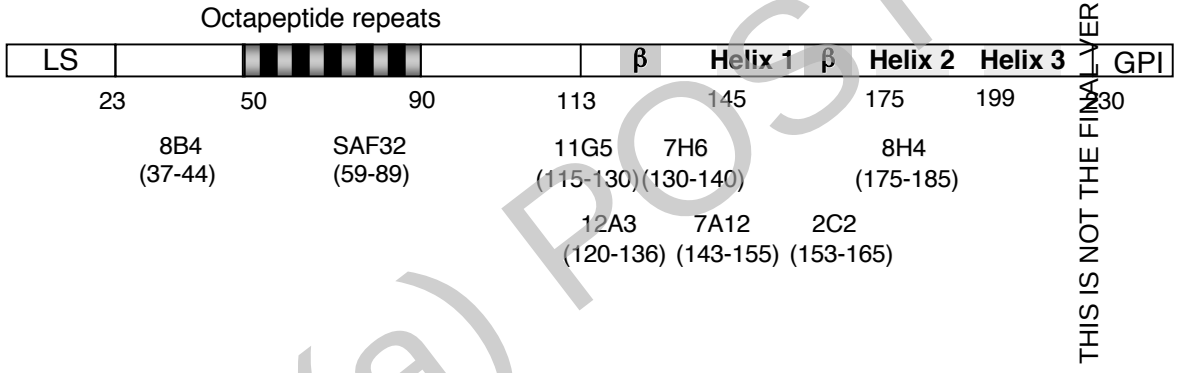

Biochemical Journal Immediate Publication. Published on 12 Oct 2007 as manuscript BJ20071122

Figure 1b. Western blot of ovine recombinant PrP

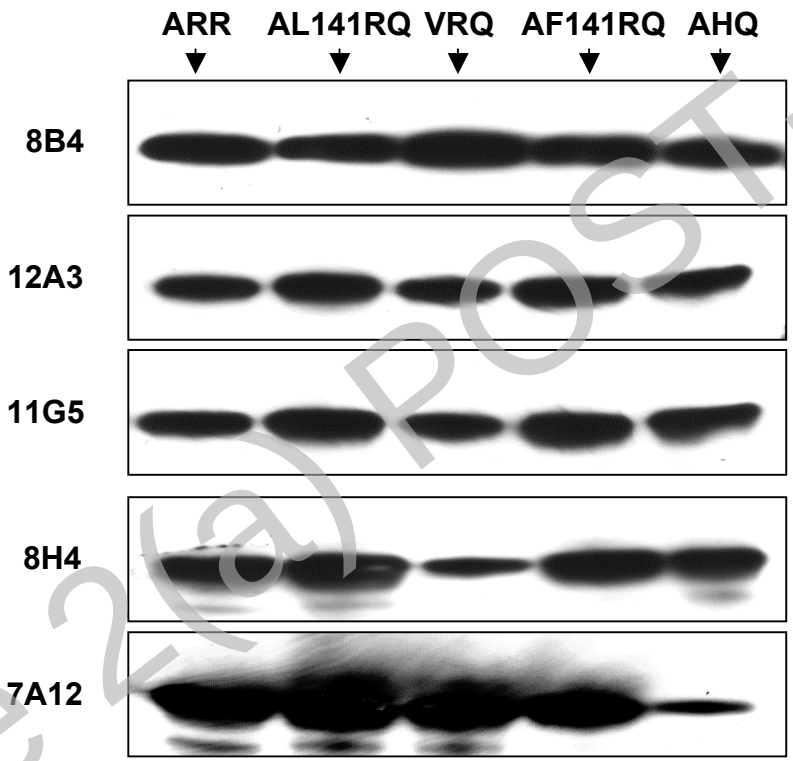

Biochemical Journal Immediate Publication. Published on 12 Oct 2007 as manuscript BJ20071122

Figure 2. Capture-detector ELISA of ovine recombinant PrP

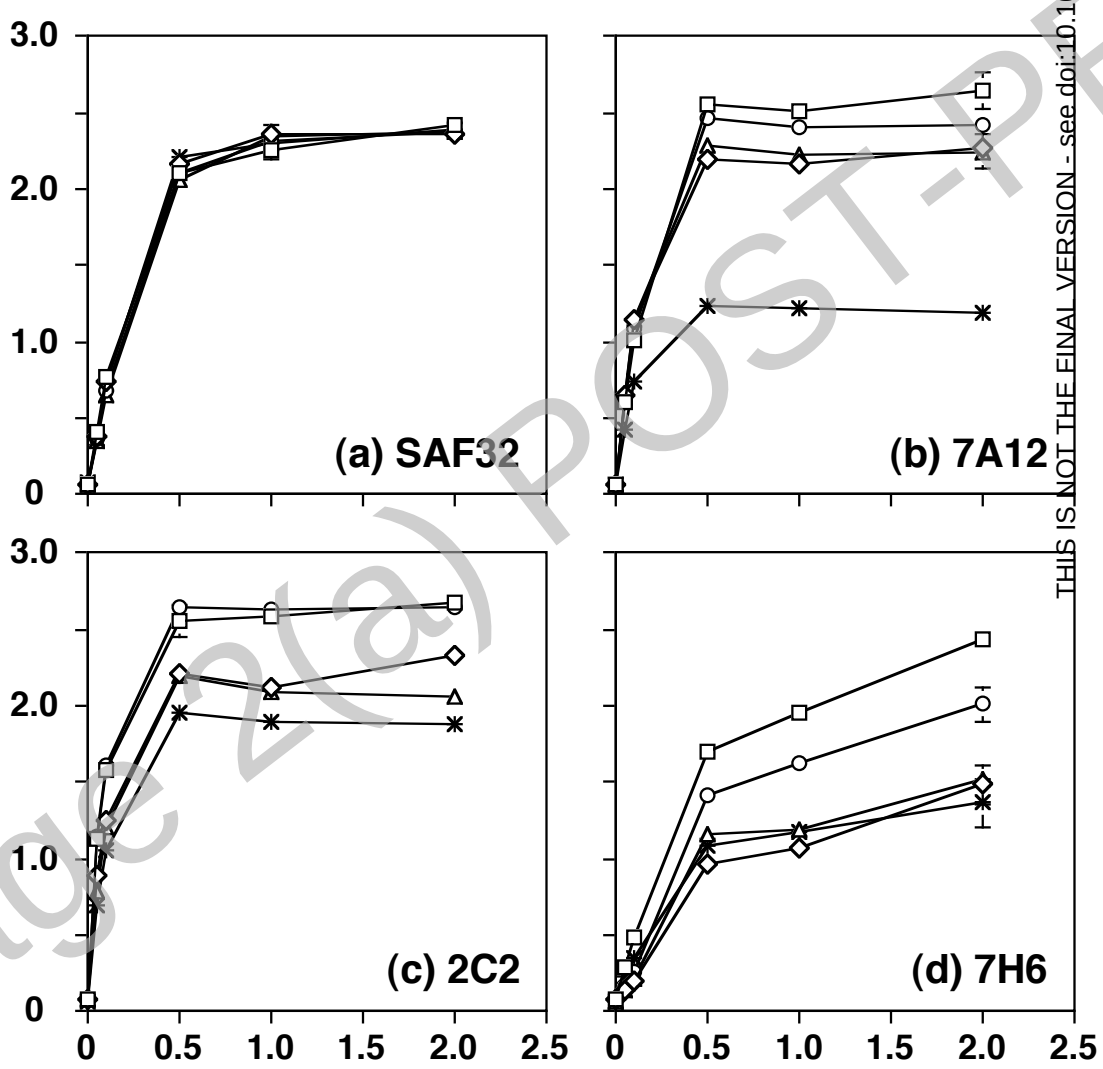

Biochemical Journal Immediate Publication. Published on 12 Oct 2007 as manuscript BJ20071122

Figure 3. Immunoreactivity of metal ion-treated ovine recombinant PrP

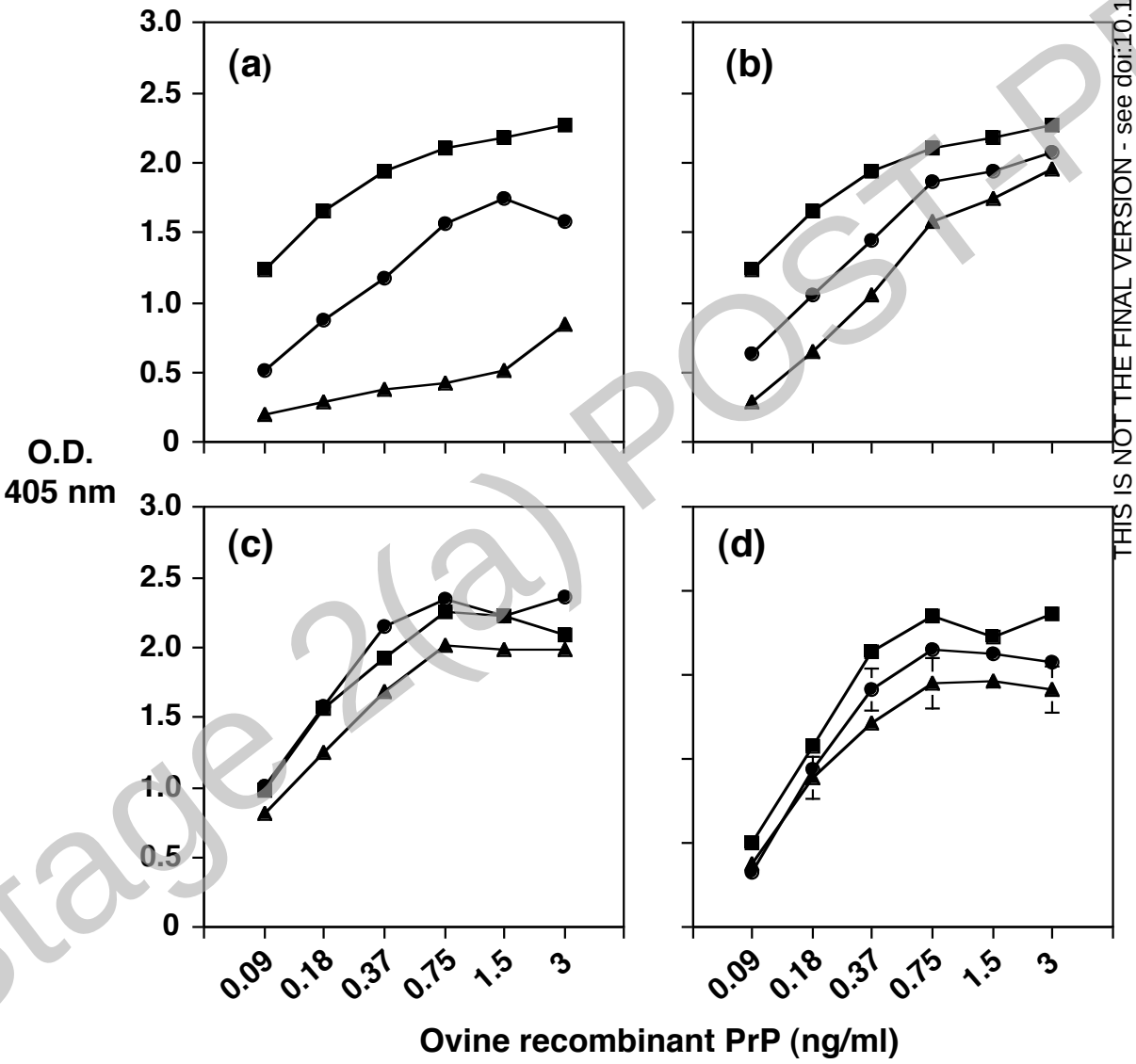

Biochemical Journal Immediate Publication. Published on 12 Oct 2007 as manuscript BJ20071122

Figure 4. Recombinant PrP aggregation assay

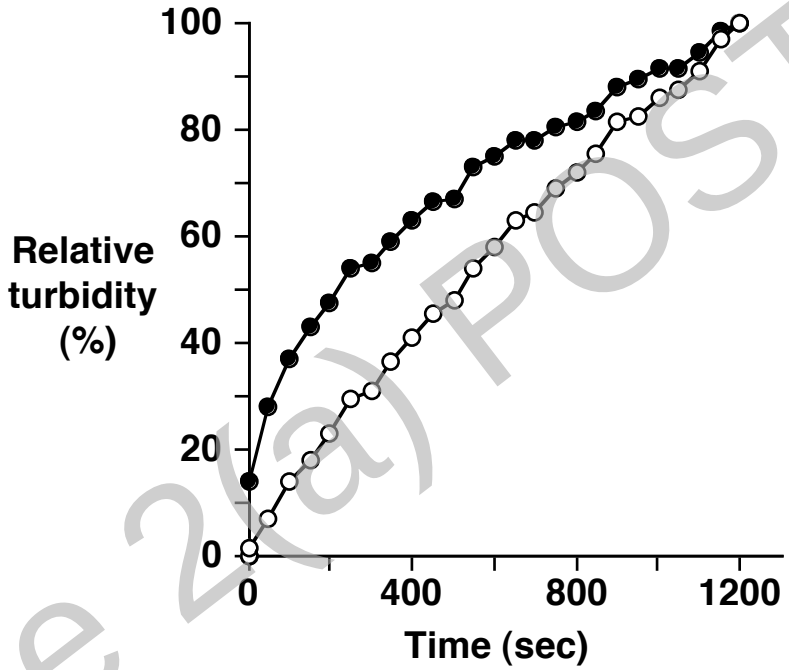

Biochemical Journal Immediate Publication. Published on 12 Oct 2007 as manuscript BJ20071122

Figure 5. Root-mean-squared fluctuations (*rmsf*) of the main-chain atoms for amino acid residues in the C-terminal region of different ovine PrP allelic variants

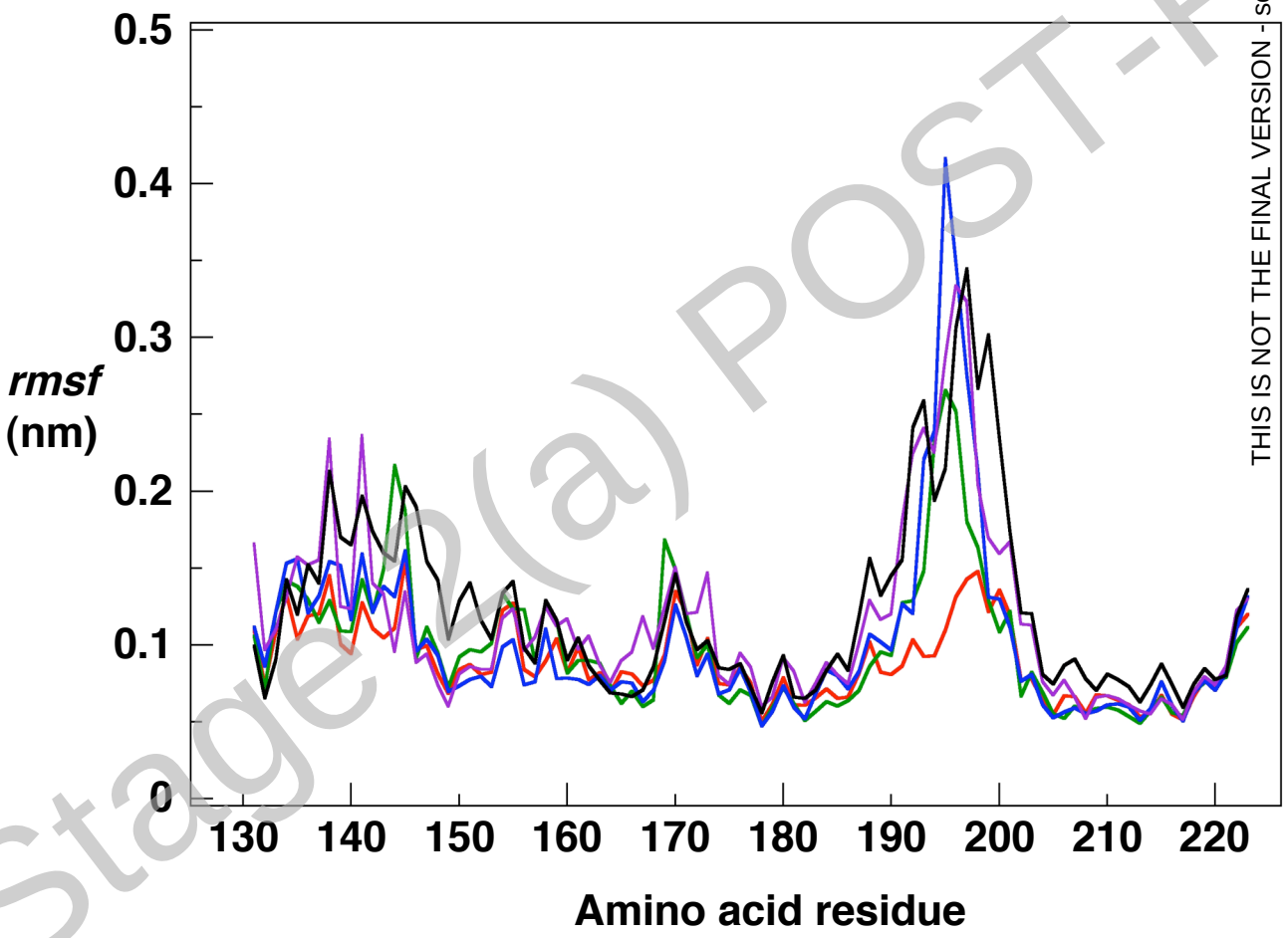

Biochemical Journal Immediate Publication. Published on 12 Oct 2007 as manuscript BJ20071122

Figure 6. Side-chain interactions in the C-terminal region of helix-2 of AL141RQ

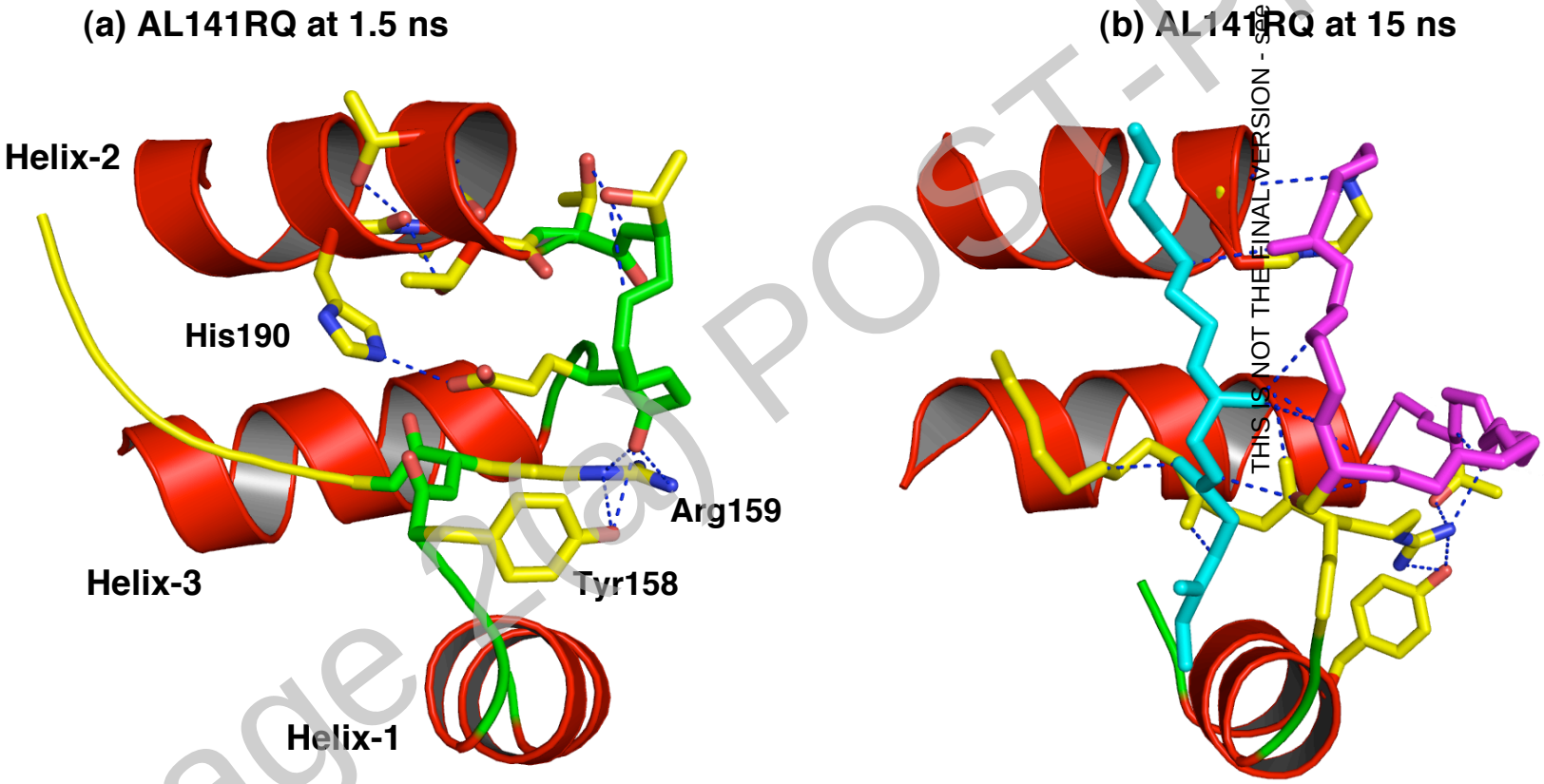

Biochemical Journal Immediate Publication. Published on 12 Oct 2007 as manuscript BJ20071122

Figure 7. Steric hindrance prevents unwinding of helix-2 in AF141RQ